UNIVERSITY OF CALIFORNIA, SAN DIEGO

# Ephrin-A1 Induces Cell Retraction to Exert Three-dimensional Traction Stress on the Substrate via a PI3K-dependent Pathway

A thesis submitted in partial satisfaction of the requirements for the degree

Master of Science

in

Bioengineering

by

Min-Shu Chan

Committee in charge:

Shu Chien, Chair
Juan Lasheras
Yu-Hwa Lo

2012

The Thesis of Min-Shu Chan is approved and it is acceptable in quality and form for publication on microfilm and electronically:

_____

_____

_____

Chair

University of California, San Diego

2012

## Dedication

This thesis is dedicated to my parents and grandparents, and sister, whose unconditional love led me to become who I am today.

## Table of Contents

## List of Figures

## Acknowledgements

I would like to express my deepest gratitude to my advisor, Dr. Shu Chien for his continuous guidance, caring, patience throughout my graduate studies. He is a great model not only in academic research but also in life. I would like to especially thank Dr. Juan Lasheras and Dr. Yu-Hwa Lo for being my committee members. Without his insights and expertise, my research would not have been possible.

I would also like to highly appreciate Dr. Julie Li, who has always been was always willing to help and give suggestions in the past year. The good advice, support and friendship of them have been invaluable on both an academic and a personal level, for which I am extremely grateful. I would like to thank everyone else in my lab. I would like to thank Dr. Sung Sik Hur and Mark Wang for always willing to share his expert knowledge and life experiences as a great researcher. I would like to thank the other lab members, Phu Nguyen, Jerry Norwich, Leona Flores, Yingli Hu, Dayu Teng, Carol Kuo, Jing Zhou, Vernon Shih for always being so accommodating, supportive, and willing to help.

As an international student in the United States, I would like to thank all of my friends in UCSD Taiwanese Graduate Student Association, especially my roommate, Yu-Hsin Liu, and my best friend, Wei-Sheng Su, for always being willing to share my laughter and tears. Without their mental support, I would not have had the

encouragement to conquer the difficulties during my graduate studies.

Last and most importantly, I would like to thank my parents and my sister. As always, home is where dream is. Even though we are in different countries, I will eternally appreciate them for being there to cheer me up and stand by me through the good time and hard time.

ABSTRACT OF THE THESIS

Ephrin-A1 Induces Cell Retraction to Exert Three-dimensional Traction Stress on the Substrate via a PI3K-dependent Pathway

by

Min-Shu Chan

Master of Science in Bioengineering

University of California, San Diego, 2012

Professor Shu Chien

The Eph family of receptor tyrosine kinases and their ligands, Ephrins, have been shown to play important roles in regulating cell migration, polarization, and cell-matrix and cell-cell adhesions. Specifically, Ephrin-A1 has been shown to regulate cell retraction via activating EphA receptors that signal to the PI3K pathway. In the current study using differential interference contrast (DIC) microscopy, Ephrin-A1 treatment of mouse embryonic fibroblasts (MEFs) caused cell edge retraction in the wild type, but not in those with PI3K subunit p85β knockout, indicating that the

Ephrin-A1 induction of cell retraction is p85β-dependent. To quantify the p85β-mediated stress generation in MEFs under Ephrin-A1 treatment, three-dimensional images of the displacement of beads embedded in the polyacrylamide substrate were acquired with confocal microscopy and determined with image processing programs, and the traction stress were computed in tangential and normal directions with finite element analysis. The results demonstrated that the tangential traction stress of wild-type MEFs increased after Ephrin-A1 treatment, while no significant change was observed in p85β-knockout MEFs. Ephrin-A1/Fc also caused the reduction of paxillin-containing focal adhesions in endothelial cell (EC) monolayer without affecting intercellular junctions; this reduction of cell-substrate attachment without affecting intercellular stress would change the stress balance and cause the uplifting of the monolayer, indicating the potential of acting as a regulator for the attachment of EC monolayer to its substrate, and thus may be applied to the coating material to guild cell attachment and migration in regulating EC behavior.

# Chapter 1 Introduction

## 1.1 Significance of Ephrins and Eph Receptors

### 1.1.1 Ephrins and Eph Receptors

The Eph receptor-Ephrin ligand system is expressed in nearly all cell types, and has been shown to be involved in many developmental processes, including the formation of cardiovascular and skeletal systems (Zimmer M. et al. 2003), by regulating cell migration and attachment that lead to the consequential proper tissue development. The Ephrin family consists of eight members and can be divided into A and B subclasses, including Ephrin-A1–A5 and Ephrin-B1-B3. Members of A subclass are linked to the membrane via a glycosylphosphatidylinositol (GPI) moiety, while the members of B subclass are anchored by a transmembrane domain and contain a cytoplasmic tail (Gale and Yancopoulos 1997). The Eph family of receptor tyrosine kinases consist of highly conserved transmembrane receptors, and they are also divided into two subclasses, i.e., EphA and EphB receptors (Pasquale 2005) according to the sequence homology of their extracellular domains. In general, EphA receptors bind to Ephrin-A ligands, while EphB receptors bind to Ephrin-B ligands. Some exceptions exist such as Ephrin-A5/EphB2 interaction and EphA4 binding to both Ephrin-A and Ephrin-B family members. Also, Ephrin-A1 largely exerts functions through interactions with EphA2.

As the major subfamily of receptor tyrosine kinases, Eph receptors interact with their surface-bound ligand Ephrin proteins to transmit intracellular and intercellular

signals. When a cell expressing Eph receptors encounters a cell expressing Ephrins, bidirectional signaling occurs between Eph receptors and Ephrins, meaning that both are components to transduce the signaling through their interaction. The forward signaling is activated by Eph receptors, while the reverse signaling is activated by Ephrins.

### 1.1.2 Eph Receptor-Ephrin Signaling in Endothelial Cells

Eph receptors and Ephrins have been shown to regulate blood vessel formation during development (Kuijper et al. 2007) and in the neovascularization of tumorigenic tissues (Castellvi et al. 2006) (Chen et al. 2006) since tumor growth requires a sufficient blood supply to support the metabolic requirements. It has been reported that Ephrin-A1 and EphA2 are both expressed in endothelial cells and tumor cells. Ephrin-A1, the ligand that has the ability to stimulate migration of endothelial cells, is shown to be a chemoattractant for endothelial cells (Pandey et al. 1995) and can induce a specific angiogenic response in rat cornea in EphA2-expressing HUVECs to stimulate vascular remodeling (Beauchamp and Debinski 2012). EphA2 receptor has been shown to regulate VEGF-induced endothelial cell capillary formation (Chen et al., 2006), and the inhibition of EphA2 prevents the morphological changes of endothelial cells required for the formation of blood vessels (Ogawa et al. 2000). It has also been reported that the blockage of the Ephrin-A1-EphA2 interaction is sufficient to inhibit new vessel growth and significantly reduces the density of tumor vasculature (Brantley et al. 2002). Altogether, Ephrin-A1 and EphA2 play an important role not only in normal angiogenesis, but also in tumor neovascularization. In my study, the effects of Ephrin-A1

on EC monolayer mechanics was investigated in order to elucidate its role in EC migration and remodelng.

### 1.1.3 Eph-Ephrin Signaling in Cytoskeletal Organization, Cell Migration, and Cell Retraction

Ephrin and Eph receptor interactions trigger the bidirectional signaling and modulate the behaviors of the contacting cells (Pasquale 2005). It has been reported that Ephrin-B2 induces the change of morphology and motility of ECs (Bochenek et al. 2010). In addition, soluble Ephrin-B1 stimulation caused the retraction and rounding of DLD1 colon carcinoma cells expressing the EphB2 receptor (Riedl et al. 2005). It has also been shown that Ephrin-A1 and EphA2 influence cell-cell and cell-ECM interaction and hence modulate cell migration. Ephrin-A1 and EphA2 interaction decreases cell attachment to ECM and integrin signaling, while increasing cell rounding and contraction in multiple cell types (Buricchi et al. 2007) (Parri et al. 2007). However, while Ephrin-A1 has been reported to induce cytoskeletal remodeling/cell rounding (Miao et al. 2000), others provide evidence that Ephrin-A1 stimulates cell adhesion and spreading (Carter et al. 2002). Such opposed results may be due to the difference in Ephrin-A1-mediated dynamics in different cell types and their varying microenvironments.

In studies on cell signaling pathway, it has been reported that Ephrin-A1-EphA2 interaction can either inhibit or stimulate the MAP/ERK kinase signaling cascade, depending on the cell type and microenvironment (Pratt and Kinch 2002) (Nasreen et al.

2007). On the one hand, it has been reported that the stimulation of MAP/ERK kinase signaling is through the ligand-activated SH2 domain of EphA2, leading to the recruitment of GRB2 and inducing the activation and nuclear translocation of ERK. The activation of ERK is accompanied by the destabilization of cell-ECM attachments in malignant mesothelioma cells (Pratt and Kinch 2002) and breast cancer cells (Nasreen et al. 2007). On the other hand, the EphA2 activation by Ephrin-A1 has been shown to inhibit the Ras/MAPK pathway in endothelial cells (Miao et al. 2001) and decrease the oncogenic signaling in PC3 carcinoma cells (Parri et al. 2005). In addition, the PI3K signaling pathway has been shown to be involved in the Ephrin-induced regulation of cell migration, filipodia formation, neuronal growth cone collapse, and cell proliferation (Hjorthaug and Aasheim 2007) (Fukushima et al. 2006) (Steinle et al. 2002, Wong et al. 2004). The association between the PI3K-p85β regulatory subunit and the cytoplasmic domain of the Eph receptor was first identified by Dixit and colleagues (Pandey et al. 1994), followed by the report for a direct link between Ephrin stimulation and PI3K enzymatic activity (Bin Fang et al. 2008). These findings place PI3K as a critical player in the Ephrin-Eph signaling pathway, as well as in the Ephrin-Eph-regulated cellular functions. It would be interesting to investigate the signaling events via PI3K pathway induced by Ephrin-A1 not only in the regulation of cell contraction, but also the formation of the boundaries between different cell types within tissues (Coate et al. 2008).

## 1.2 The Measurement of 3D Traction Force Exerted by Cells

### 1.2.1 Cell Traction Force

Cell traction force (CTF), the tension of contracting cell body that exerts on ECM, is generated by actomyosin crossbridges inside the actin filaments-forming semi-sarcomere structure through ATP hydrolysis and then transmitted to the ECM (Wang and Lin 2007). CTF can also be generated by actin polymerization, which usually occurs at leading edge of the migrating cell (Bereiter-Hahn 2005, Elson et al. 1999). The cytoskeleton is connected to the ECM to relay traction forces to ECM through FAs, which is the assembly of ECM proteins, transmembrane receptors, and cytoplasmic structural and signaling proteins that are located at the ends of the actin stress fibers and the ECM (Burton and Taylor 1997, Lee et al. 1994, Tan et al. 2003). CTF is modulated by the molecules that regulate the assembly of stress fibers and FAs including Rho-kinase/ROCK (Watanabe et al. 1999) and molecules that regulate non-muscle myosin II such as MLCK (Hartshorne et al. 1998). CTF is essential for not only cell migration but also signal generations and cellular functions in many biological processes such as inflammation, wound healing, embryogenesis, angiogenesis, and metastasis. Thus, the regulation of CTF plays an important role in physiological events of tissue and organ. Our previous results demonstrated that Ephrin-A1/Fc caused the activation of Rho-ROCK pathway, actin stress fiber formation, and focal adhesion de-phosphoyrlation (Fero 2008). It is not clear if those Ephrin-A1/Fc-caused cellular changes transmitted to CTF generation. In the current study, I investigated the effects of Ephrin-A1/Fc on CTF

in three different cell types, wild type and p85β-KO MEFs, and bovine aortic EC monolayer.

### 1.2.2 Traction Force Measurement

Several methods can be used to measure CTF with various forms of transparent flexible substrate. These methods are based on the determination of substrate deformation induced by the cell retraction. In general, there are several methods developed depending on the characteristics of the substrates such as Wrinkling Silicone Substrate Method, Micropatterned Silicone (PDMS) Substrate Method, Cantilevers Methods, and Polyacrylamide (PAA) Method.

A.K. Harris and colleagues developed the Wrinkling Silicone Substrate Method to measure the CTF of chicken heart fibroblasts on thin silicon rubber film by calculating the surface wrinkle caused by the cell contractile forces (Harris et al. 1980). Afterward, Burton and colleagues improved the approach using ultraviolet light to control the substrate stiffness which allowed high wrinkle density and thus increase the sensitivity and resolution CTF (Burton and Taylor 1997). The contractile forces were then estimated by multiplying the number of wrinkles and the substrate stiffness (Burton et al. 1999). However, the winkle-based CTF measurement still has many limitations in quantifications and resolutions.

Micropatterned silicone (PDMS) substrate method is one of the improved methods which are based on the non-wrinkling silicon substrate method (Bershadsky et al. 2003). Silicon (Si) or gallium-arsenic (GaAs) molds were used to print the micropatterned PDMS elastomer substrate. The control of the mechanical properties of the substrate and regularity of its pattern made it easier for direct visualization and calculation of the contractile strain exerted by the cells. However, the micropatterns could also affect cell adhesion and migration through contact guidance, which cannot represent the continuous substrate surface that cells encounter in the physiological conditions (Weiss and Moscona 1958).

Tan and colleagues developed the method for CTF measurement based on the calculation from the deflection of vertical cantilevers molded in the PDMS elastomer via lithographic technique (Tan et al. 2003). The magnitude and direction of the CTF were measured by the deflection of cantilevers since they move independently, but this method has limitation in spatial resolution.

During 1997, Pelham and colleagues used polyacrylamide (PAA) substrate to measure CTF of migrating cells for the first time. The stiffness of the substrate was controlled by adjusting the concentration of crosslinkers, and the CTF exerted by the cells was measured by the displacement of the fluorescent beads embedded in the deformable PAA (Kaverina et al. 2000). PAA exhibits better mechanical and optical properties comparing with silicone for observing and calculating CTF. Since cells have low affinity

to PAA, coating PAA with various ECM via chemical approaches will allow better controls of cell adhesions. While the substrate is easy to prepare, due to the continuity of the substrate, it also has some disadvantage such as additional image processing and traction force computational procedures. Butler and colleagues developed the method to compute the CTF field by recasting the relationship between displacement and CTF into Fourier space (Butler et al. 2002). del Alamo and colleagues also developed the quantitative approach to study the differences in migrating mechanics of cells moving up a chemoattractant gradient by providing the solution of the elastostatic equation based on Fourier expansions that express the CTF as a function of deformation (del Alamo J. C. et al. 2007). Furthermore, the finite thickness of the substrate was taken into account to increase the accuracy of Boussinesq solution and allow for non-zero net forces. The effect of the distance between the measurement plane and the surface of substrate was also taken into consideration to refine the solution.

Since cells are 3D in shape and can sense and respond to the 3D geometry in their environment, it is reasonable to expect that a cell can exert forces in all directions, but all 2D methods mentioned above have the implicit assumption that adherent cells on 2D substrate do not apply forces in normal (Z) direction perpendicular to substrate (i.e., Tz=0). Our lab has developed novel methods for computing CTF in 3D based on finite element method (FEM) and demonstrated that ECs apply forces in the normal direction as well as tangential (XY) directions (Hur et al. 2009). Study based on fast Fourier

Transform have also verified that migrating amoeboid cells show traction force behavior in 3D (del Alamo Juan C. et al. 2010).

In my study, I have employed the novel method based on image processing and FEM to measure traction stress of retracting cell induced by enprhin-A1/Fc.

# Chapter 2 Materials and Methods

## 2.1 Cells and Cell Culture

The mouse embryonic fibroblast cells (MEFs) derived from pik3R2-/- knockout mice (Brachmann et al. 2005) and bovine aortic endothelial cells (BAECs) isolated from the bovine aorta with collagenase (Li S. et al. 1999) were used in the experiments.

The MEFs were cultured in Dulbecco's modified Eagle's medium (DMEM) (GIBCO-BRL, Gaithersburg, MD) supplemented with 15% fetal bovine serum (FBS) (GIBCO-BRL), 1% penicillinstreptomycin,1% L-Glutamine, and 1% sodium pyruvate. Bovine aortic endothelial cells were cultured in Dulbecco's modified Eagle's medium (DMEM) (GIBCO-BRL, Gaithersburg, MD) supplemented with 10% fetal bovine serum (FBS) (GIBCO-BRL), 1% penicillinstreptomycin,1% L-Glutamine, and 1% sodium pyruvate. All cell cultures were maintained in a humidified incubator at 37°C with 5% $CO_2$.

## 2.2 Biologic Reagent

For experiments where cells were treated with recombinant mouse Ephrin-A1/Fc (R&D Systems) in the medium, it was added at a final concentration of 2μg/mL in DMEM.

## 2.3 Preparation of Polyacrylamide Deformable Substrate

Polyacrylamide deformable substrate was prepared as described below, based on the method developed by Yuli Wang and colleagues (Pelham and Wang 1997). The preparation steps include the activation of glass-bottom dishes, polymerization of substrate including the fluorescent beads, and ECM protein coating on the surface of the substrate.

The bottom surfaces of glass-bottom dishes were activated with inner flame using a Bunsen burner to make it hydrophilic. The 0.1 M sodium hydroxide (NaOH, Merck & Co., Inc., Whitehouse Station, NJ) was added on the surface and air dried, then it was siliconized with 3-aminopropyl triethoxy silane (Sigma-Aldrich Co., St. Louis, MO) followed by activation with 0.5% glutaraldehyde (Sigma), which made the formation of covalent bonds between glass surface and polyacrylamide. The dishes with activated glass surface were then stored in desiccators prior to polyacrylamide gel preparation.

For polymerization of the substrate, the monomer solution was prepared with acrylamide (40% w/v, Bio-Rad Laboratories, Inc, Hercules, CA), N,N'-methylene bis-acrylamide (bis-acrylamide) (2% w/v, Bio-Rad), 4-(2-hydroxyethyl)-1-piperazineethanesulfonic acid (HEPES) buffer (1 M, pH 8.5, EMD Chemicals Inc., Gibbstown, NJ), 0.2-μm diameter red (580/605) fluorescent polystyrene beads (FluoSpheres, Molecular Probes/ Invitrogen Corp., Carlsbad, CA), and distilled water. The final concentration was 10% for acrylamide (monomer) with 0.1% bis-acrylamide in

order to control the rigidity. Young's Modulus was determined to be 9.0 kPa by atomic force microscopy (AFM) (Hur et al. 2009). The fluorescent beads were sonicated for 5 min in the ultrasonic sonicator (BANSONIC®, BRANSON ULTRASONICS Corp., Danbury, CT) to disperse the aggregates, and then added into the monomer solution. The solution was thereafter syringe-driven through 0.22-μm filters (MILLEX, Millipore Corp., Billerica, MA) to remove the remaining aggregated beads. Polymerization started while 0.06% ammonium persulfate (APS, SIGMA) and 0.4% N,N,N',N'-tetramethylene diamine (TEMED, Invitrogen) were added to the monomer solution. APS is an initiator and TEMED is a catalyst for the polymerization. The solution was dropped onto the surface of glass bottom dishes, covered with inactivated glass coverslips (diameter 18mm), and then allowed to polymerize for 40 min at room temperature.

The polyacrylamide gels were conjugated with the ECM protein bovine fibronectin (FN, SIGMA) to allow the adhesion of MEFs and ECs. N-Sulfosuccinimidyl-6-[4'-azido-2'-nitrophenylamino] hexanoate (Sulfo-SANPAH, Pierce Biotechnology, Rockford, IL) was added onto the polymerized polyacrylamide substrate and activated by ultraviolet (UV) light in order to couple the phenylazide group of polyarylamide and the sulfosuccinimidyl group of FN, which was spread on the substrate at a concentration of 100 μg/mL diluted in phosphate buffered saline (PBS). The FN-coated polyacrylamide substrates were incubated overnight at 4°C before cell seeding.

## 2.4 Live Cell Imaging

FN-coated polyacrylamide substrates were exposed to UV light (SPECTROLINE, Spectronics Corp., Westbury, NY) for 10 minutes in order to keep the microbial contamination under control, with the aid of antibiotics (penicillin-streptomycin). After the substrate had been equilibrated with the growth medium at $37^{o}$C for 1 hour, cells were seeded on the substrates and allowed to adhere/spread for 24 hours in low-serum medium (0.5% FBS). Before imaging, the medium was replaced by fresh low-serum medium.

A spinning disk confocal microscope (IX-81, Olympus, Olympus America Inc., Center Valley,PA) with a 60X objective lens (UIS Plan-Apo, N.A. 1.40, Olympus) was used to acquire images of cells and substrate. DIC technique was employed for cell imaging, and fluorescent confocal imaging technique was used to acquire the images of imbedded marker beads. The magnification scale was 0.1075 μm / pixel in X,Y directions, and the optical section step was 0.2 μm. “Force-loaded” images were acquired from the bead-embedded gel on which the cells were attached and exerted their traction force. The “Null-force images” were taken from the gel without the cells following their removal with trypsin-EDTA (Sigma) to eliminate the cell-induced gel deformation.

The cells were stimulated with Ephrin-A1/Fc, and one field of view was imaged over a continuous 40-minute time course with a charge-coupled device (CCD) camera (ORCA-II-ER, Hammamatsu Photonics K.K., Hamamatsu, Shizuoka, Japan) and MetaMorph image acquisition software (Molecular Devices, Corp., Downingtown, PA).

The temperature ($37^{o}$C) and $CO_2$ concentration (5% CO2-95% air) were controlled during the imaging process.

## 2.5 Determination of 3D Displacement and Stress

In order to reconstruct the substrate deformation, the image processing programs coded in MATLAB was used. 3D displacements were determined by dividing each 3D "Force-loaded" image and comparing it with corresponding "Null-force" image in 3D interrogation boxes. We then calculated the correlation function between pairs of boxes and found the displacement that maximizes the correlation (del Alamo Juan C. et al. 2010).

After getting the 3D displacements, boundary value problems (BVPs) were defined to determine stress field. The polyacrylamide substrate is assumed to be an isotropic elastic material, which means that the mechanical property can be described with two mechanical parameters, i.e, the Young's Modulus and the Poisson's ratios. Elasticity of polyacrylamide was verified in previous studies (Hur et al. 2009). Young's modulus was measured as 9.0 kPa by AFM. 0.3 was used as a value of Poisson's ratio as in previous study (Li C. et al. 1993).

The governing equations are as following.

(1) The strain-displacement equation:

$$\varepsilon_{ij} = \frac{1}{2}\left(\frac{\partial u_i}{\partial x_j} + \frac{\partial u_j}{\partial x_i} + \frac{\partial u_k \partial u_k}{\partial^2 u_i u_j}\right)$$

Where $\varepsilon_{ij}$ is the stain tensor (i, j= 1,2,3), $u_i$ is the displacement vector, and $x_i$ is the Cartesian coordinates (i=1,2, 3).

(2) The elastic stress-strain law (Hooke's Law):

$$\varepsilon_{ij} = \frac{1}{E}\{(1+v)\sigma_{ij} - v\delta_{ij}\delta_{kk}\}$$

Where $\varepsilon_{ij}$ is the stress tensor, $E$ is Young's modulus, $v$ is Poisson's ratio, and $\delta_{ij}$ is Kroneker delta.

(3) Quasi-static equilibrium

$$\frac{\partial \sigma_{ij}}{\partial x_i} = 0$$

The domain of the BVP is set within the ends in direction x at x=0 and x=$X_L$ and in direction y at y=0 and y=$Y_L$. The top of the polyacrylamide substrate where the cell is attached is set at z=$Z_L$ in z direction, while the bottom of the substrate attaching to the glass bottom dish is set as z=0 (Figure 1). Boundary conditions are applied to solve BVPs; $u_i = 0$ at $z = 0$, meaning that there is no displacement of the beads on the gel bottom, and $u_i = u_i^*$ at $z = Z_L$, where $u_i^*$ is the measured displacement at the top plane of the gel.

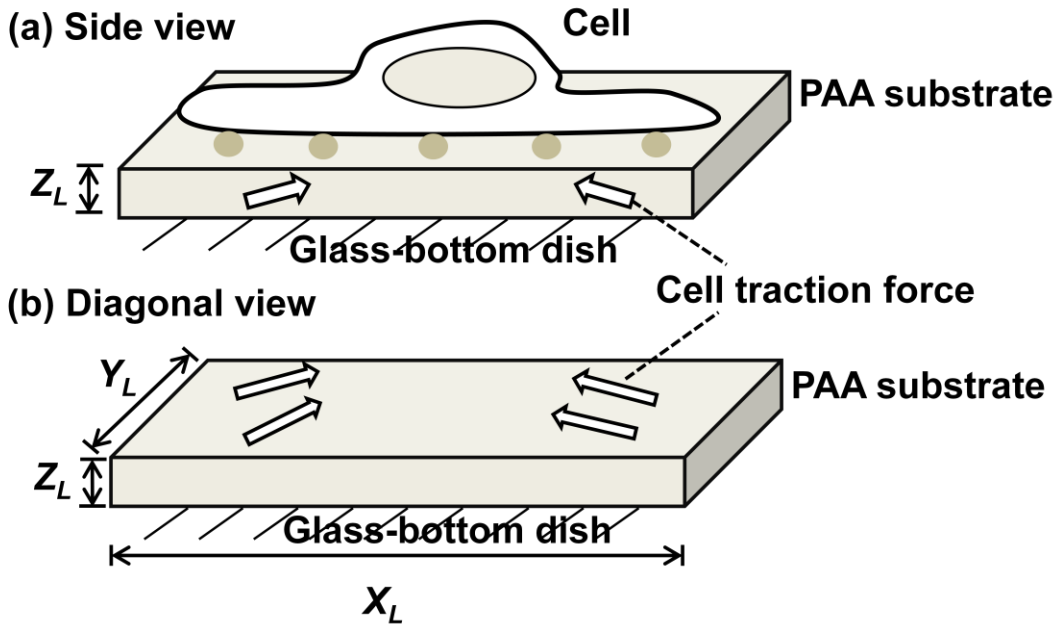


Figure 1. Schematic diagram showing a cell applying forces on the deformable PAA substrate attached on the glass surface. (a) A cell exerts traction forces onto underlying PAA substrate. (b) The deformable PAA substrate with cell traction forces. $X_L$, $Y_L$, $Z_L$: the dimensions of PAA domain for the analyses in *X*-, *Y*-, and *Z*-directions, respectively.

The FEM was then used to calculate the 3D traction stress solving BVPs as formulated above. FEM is a common technique used for constructing a computational solution for BVPs. By dividing the domain of the solution into a finite number of sub-domains (the finite elements), the approximation of solution can be constructed with the collection of finite elements using variation concepts (Becker and Waller 1986). In this study, we used the hexahedron (brick) type element, which has 8 nodes at the corner and eight Gauss integration points inside. Fixed mesh grids of 3.44 μm were used in all X, Y and Z directions. ABAQUS 6.5 (SIMULIA, Providence, RI), a commercial software package for FE analysis, was used to solve BVP.

## 2.6 Immunostaining and Fluorescence Microscopy

The focal adhesions and junctions of EC monolayer were observed using immunostaining of Paxillin and β-catenin, respectively, followed by fluorescence microscopy with or without Ephrin-A1/Fc treatment. Confluent ECs were plated on a glass-bottom dish followed by cell starvation with 0.5% serum-containing medium for 24 hours, and then the cells were treated with 2μg/mL Ephrin-A1/Fc for the indicated time periods. The cells were then washed three times with PBS at room temperature, fixed for 15 minutes with 2.5% paraformaldehyde, permeabilized with 0.1% Triton X-100 in PBS, and blocked for 1 hour with 5% bovine serum albumin (BSA) in PBS. After blocking, the cells were incubated with primary antibodies against Paxillin or β-catenin (Cell Signaling) for 3 hours at room temperature at a concentration of 1:200 in 5% BSA in PBS, washed three times with PBS for 15 minutes each, and incubated with a FITC-conjugated anti-mouse IgG secondary antibody (Jackson Immunoresearch, at a concentration of 1:200 in 5% BSA in PBS) for 1 hour at room temperature. The FITC staining was then observed with fluorescence microscopy with excitation at a wavelength of 488 nm and detection between 506 and 538 nm. The Images were captured with IP Lab image acquisition software.

## 2.7 Statistical Analysis

Analysis of variance (ANOVA) was used to test the differences between multiple groups. When a difference was detected, the Tukey's honestly significant difference test was used to determine which groups differ through pair-wise comparisons. If multiple

groups were not involved, then a Student t-test was used to determine statistical significance between two groups. In the statistical analysis, those with a p-value less than 0.05 were considered statistically significant.

# Chapter 3 Results

## 3.1 Traction Stress Analysis of MEFs- Startup Experiment

The live cell microscopic studies were performed in a climate-controlled hood, with a constant temperature of 37$^{o}$C and a gas environment of 5% $CO_2$-95% air. I did a time course experiment to determine the duration needed for cells to stabilize after their transfer from the incubator before performing the Epherin-A1/Fc experiments.

As shown in Figure 2, the traction stress showed no significant changes over the 120-minute which is the time course after cell transfer from the incubator, suggesting that the traction stress exerted by live cells were stable while adapting to the environmental changes during this period. To control the starting time point of my experiment, the Epherin-A1/Fc treatment was performed after a 20-minute period of time for instrument settling and microscopy adjustment. In the studies reported below, 0 time refers to the time after the elapse of the 20 minutes after cell transfer from incubator.

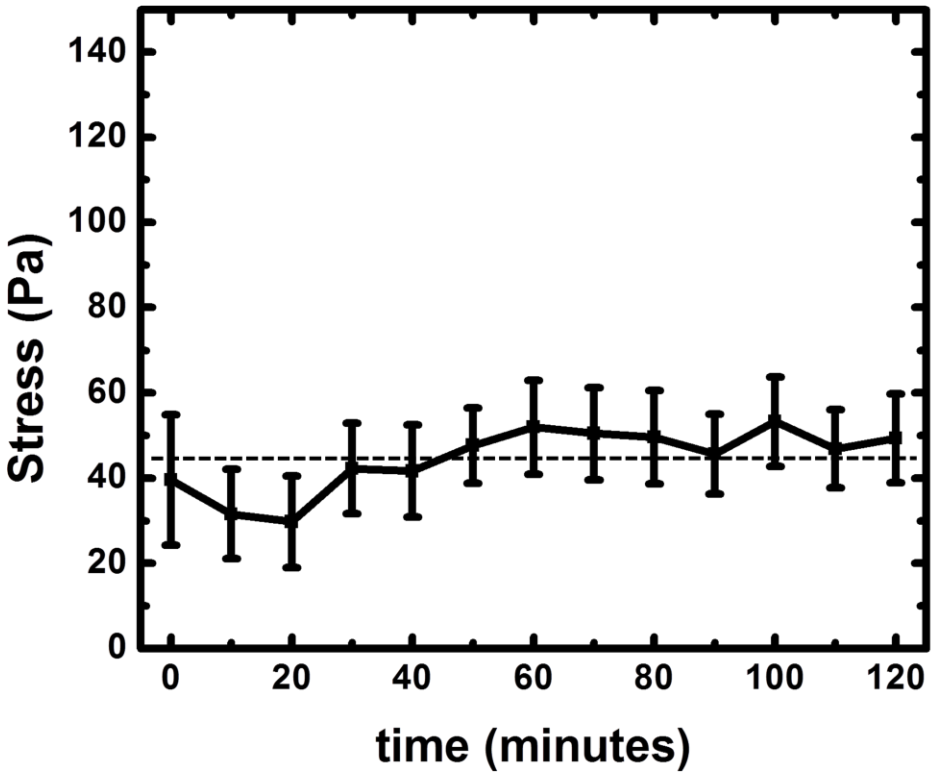


Figure 2.Quantification of the traction stress exerted by wild type MEFs over two hours based on the displacement of beads embedded in the polyacrylamide gel. There is no significant difference in the time points during this 120-minute period.

## 3.2 Ephrin-A1/Fc Induces Cell Retraction in Wild Type MEFs

To determine the Ephrin-A1-induced morphological changes in MEFs, the wild type MEFs were treated with Ephrin-A1/Fc 20 minutes after cell transfer from the incubator (Section 3.1), and the live-cell bright field images were acquired thereafter over a 30-minute time course to investigate the changes in cell morphology and spreading area by tracking the cell boundaries as a function of time. As shown in Figure 3, the wild type MEFs exhibited a morphological change within 10 minutes following Ephrin-A1/Fc-treatment, the cells retracted their protrusions and decreased their cell area (panel b). The retraction process continued at 20 and 30 minutes after the Ephrin-A1/Fc treatment (panel d), as seen by the rounded and retracted morphology, as compared with that at zero time (panel a). The two-dimensional cell areas were measured and plotted over time (Figure 4). The area of MEFs decreased after being treated with Ephrin-A1/Fc (red) in comparison with the control treated with Fc fragment (black) and the values were significantly different from control at 20 and 25 minutes ($p<0.05$).

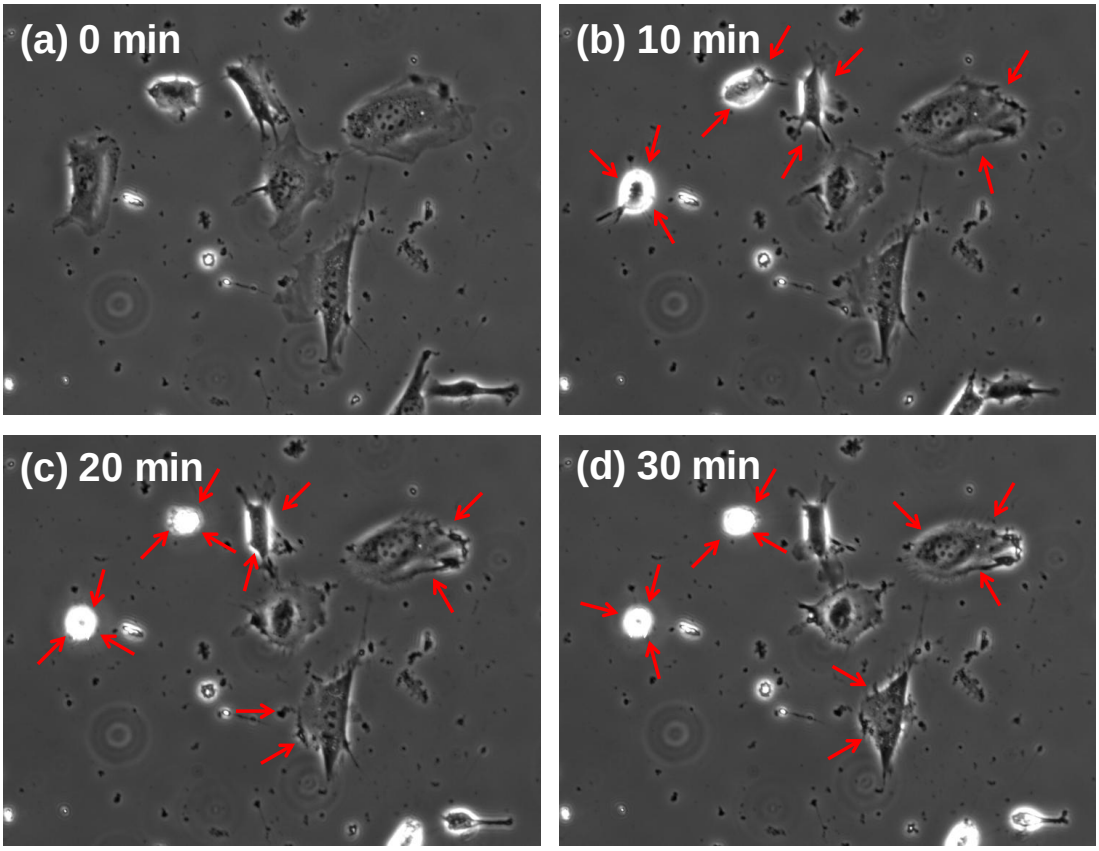


Figure 3. Morphological changes of wild type MEFs induced by Ephrin-A1/Fc. Wild type MEFs were treated with 2μg/mL Ephrin-A1/Fc, and time-lapse DIC microscopy was performed at indicated time periods to acquire the cell images. The sites of retraction induced by Ephrin-A1/Fc are indicated by arrows (panels a-d).

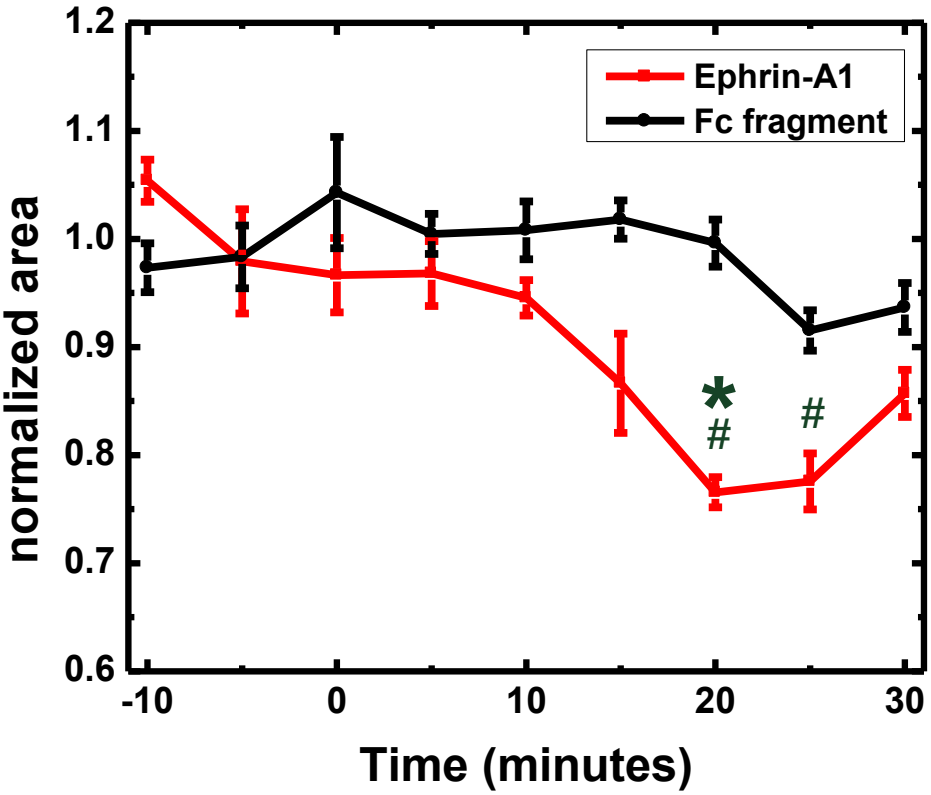


Figure 4. Changes of cell area of the wild type MEFs treated with Ephrin-A1/Fc and control Fc fragment quantified over time. The treatment was performed 20 minutes after cell transfer from the incubator, and the cell area was determined by measuring the pixel numbers within the cell boundary. * indicates $p<0.05$ at the specific time point compared with corresponding control (Ephrin-A1/Fc vs. control Fc fragment), and # indicates $p<0.05$ compared with the value at time zero under the same treatment. The values were normalized with the mean values from the first three time points before Ephrin-A1/Fc treatment.

## 3.3 Ephrin-A1/Fc Induces Traction Stress Generation in Wild Type MEFs

In order to further characterize the Ephrin-A1/Fc-induced cellular responses which was performed 20 minutes after cell transfer from the incubator (Section 3.1), the displacements of the fluorescent beads embedded in the substrate were tracked in tangential ($D_{xy}$) and normal ($D_z$) directions in order to calculate the traction stress related to morphological changes of MEFs. Figure 5 shows the total magnitude of bead displacement before (panel b) and after (panel d) treatment with Ephrin-A1/Fc, respectively, corresponding to the respective bright-field images of MEFs (panels a and c). The traction stresses exerted by the cells in tangential ($T_{xy}$) and normal ($T_Z$) directions were calculated based on strain-displacement equation (Section 2.5) to demonstrate the total magnitude of stress. The traction stress in tangential direction ($T_{xy}$) was dominant, and the stress in normal direction ($T_Z$) was much lower; This is likely due to the direction of stress fibers being in the direction of the long axis of the cell during contraction (Fero 2008). Before the treatment with Ephrin-A1/Fc, the cell exhibited a modest traction stress with small magnitudes of bead displacements distributed mainly at the edges of the cells without a clear direction (panel b) as the cell moves randomly. Ephrin-A1/Fc induced a marked cell retraction as shown by the larger bead displacements, especially at cell edges (panel d). As shown in figure 6, Ephrin-A1/Fc caused an increase in traction stress exerted by cells to reach a peak value at 10 minutes that was significantly higher than the value before Ephrin-A1/Fc treatment ($p<0.05$). The 10-minute value under Ephrin-A1/Fc treatment was also significantly higher than that of the corresponding time-matched control ($p<0.05$).

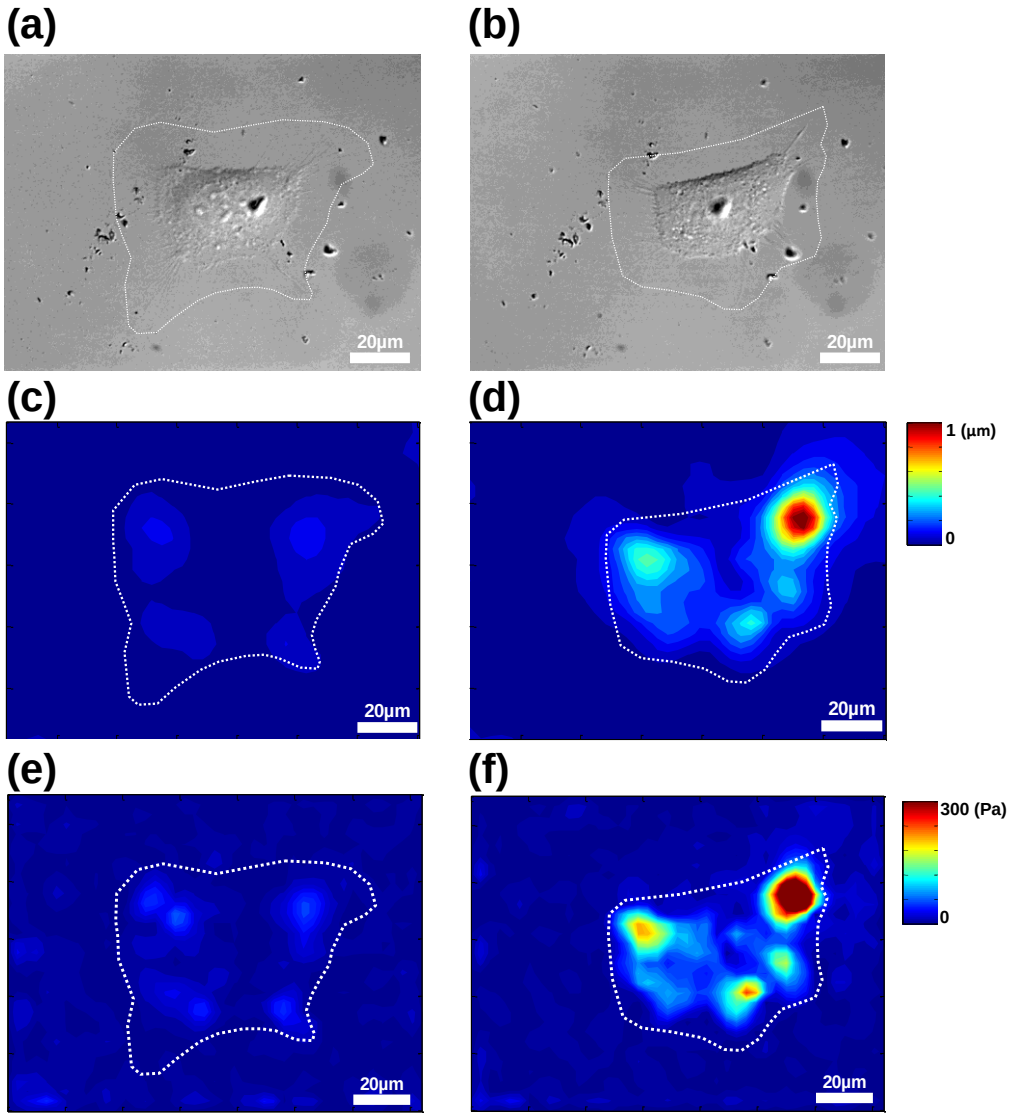


Figure 5. Mapping of MEF retraction induced by Ephrin-A1/Fc. (a) and (b): Bright-field images of a wild type MEF before (a) and 30 minutes after (b) Ephrin-A1/Fc treatment (2 μg/mL). (c) and (d): Bead displacement fields around the cell before (c) and 30 minutes after (d) Ephrin-A1/Fc treatment. (e) and (f): Traction stress exerted by wild type MEF before (e) and 30 minutes after (f) Ephrin-A1/Fc treatment (2 μg/mL). The cell boundaries drawn from the bright-field images (a and b) are shown as white lines in panels (c)-(f), respectively. Color scales in (b) and (d) indicate the total magnitudes of displacement.

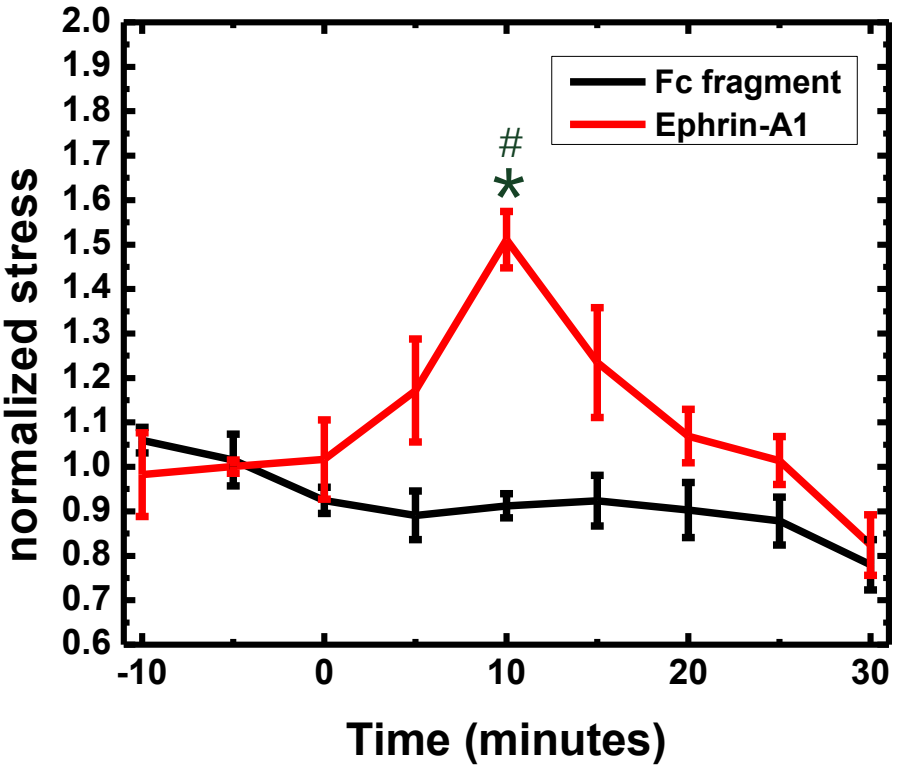


Figure 6. The magnitudes of traction stress exerted by wild type MEFs treated with Ephrin-A1/Fc and control Fc fragment. They were quantified over time was based on the bead displacement fields described in Figure 5 (panels d vs. c). * indicates $p<0.05$ at the specific time point compared with corresponding control (Ephrin-A1/Fc vs. Fc fragment treatment), and # indicates $p<0.05$ compared with the value at time zero under the same treatment. The values were normalized with the mean values from the three time pointsbefore Ephrin-A1/Fc treatment.

## 3.4 Ephrin-A1-Induced Cell Retraction and Traction Stress Generation Are PI3K-p85β-dependent

It has been shown that the cell migration and receptor-ligand complex endocytosis are regulated by the interaction between Eph receptors and PI3K (Pandey et al. 1995) (Kinch et al. 2003) (Zhuang et al. 2007). The Ephrin-regulated cell retraction may be involved in regulation of the cell functions such as repulsion and migration. Thus, I hypothesized that the Ephrin-A1/Fc-induced cell retraction is mediated through PI3K pathway. To determine the roles of PI3K subunits in regulating ephrinA1-induced cell retraction, the MEFs from p85β knockout mice were used for experiments. The wild type MEFs responded to Ephrin-A1/ Fc treatment with significant cell retraction and an increase of traction stress (figures 7-9). In contrast, the p85β-/- MEFs did not respond to the Ephrin-A1/Fc treatment. These results provide new insight of the specificity of Ephrin-A1 signaling events through the p85β-/- subunit.

### 3.4.1 Ephrin-A1/Fc-induced Morphological Change is PI3K-p85β-dependent

To investigate the differences in Ephrin-A1/Fc-induced cell retraction between wild type and p85β-/- MEFs, live-cell imaging DIC microscopy was used to acquire the cell morphology in real time. The wild type MEF exhibited cell retraction 20 minutes after Ephrin-A1/Fc treatment (Figure 7, panels e-f). In contrast, p85β-/- MEF exhibited no morphological change after treatment with Ephrin-A1/Fc (panels a-d). The plot of 2-dimensional cell areas over time in Figure 8 shows that the cell area of wild type MEFs

significantly decreases after the Ephrin-A1/Fc treatment at 20 and 25 minutes ($p<0.05$). This was followed by cell re-spreading with the emergence of lamellipodia and increase in cell area 30 minutes after the Ephrin-A1/Fc treatment.

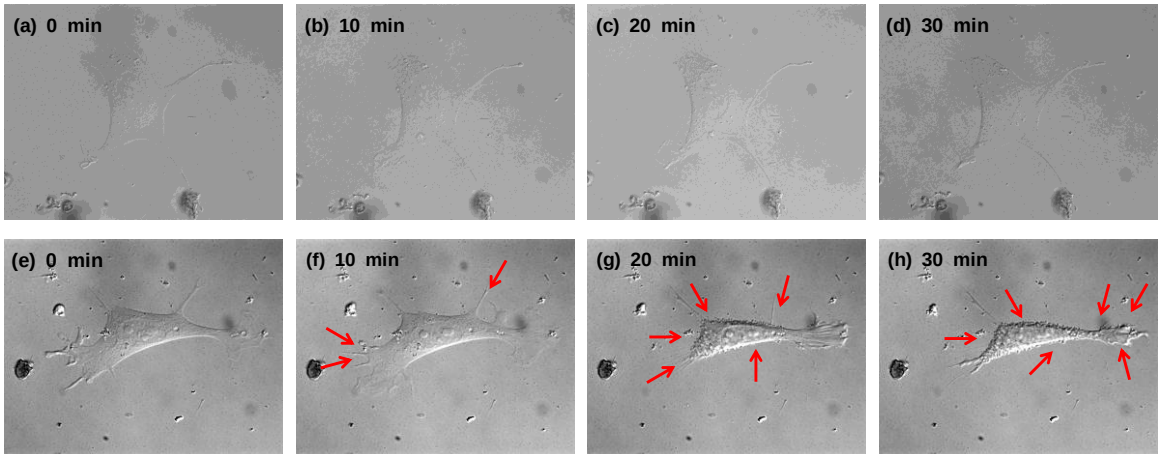


Figure 7. Ephrin-A1/Fc-induced cell retraction is PI3K-p85β-dependent. p85β -/- (a-d) and wild type (e-h) MEFs were treated with 2µg/mL Ephrin-A1/Fc for the indicated time periods, and time-lapse DIC microscopy was performed. The wild type MEFs showed significant retraction at cell edges, but p85β -/- did not show any morphological change over time.

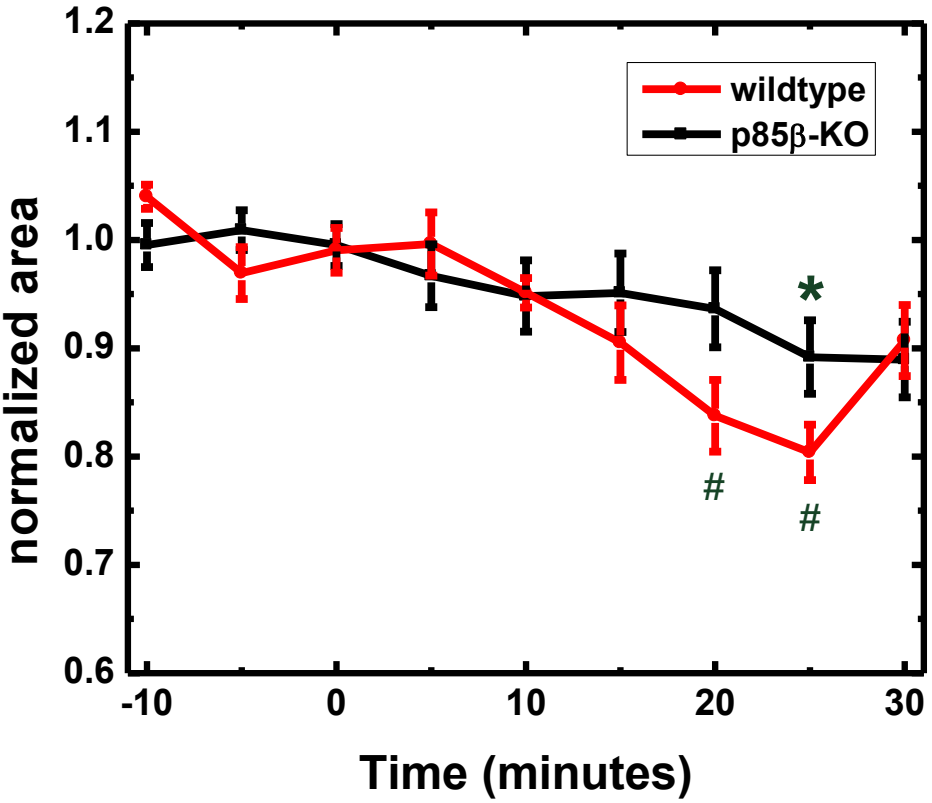


Figure 8. The cell areas of wild type and p85β-/- MEFs treated with Ephrin-A1/Fc. They were quantified over time, based on 2-dimesional pixel area. * indicates $p<0.05$ at the specific time point compared with the corresponding control (p85β-/- vs. wild type MEFs), and # indicates $p<0.05$ compared with the value at time zero of the same cell type. The values were normalized with the mean values from the three time points before Ephrin-A1/Fc treatment.

### 3.4.2 Ephrin-A1/Fc-induced Traction Stress Generation is PI3K-p85β-dependent

To quantify the differences of traction stress following Ephrin-A1/Fc treatment of wild type vs. p85β-/- MEFs, these cells were seeded on substrates with the embedded florescent beads, and beads displacements were tracked over 30 minutes (Figure 9). Ten minutes after Ephrin-A1/Fc treatment, the traction stress of wild type MEF was significantly higher than that before treatment and also that of the p85β-/- MEFs, which showed relatively steady traction stress that was not significantly affected by Ephrin-A1/Fc treatment. These results suggest that the knockout of PI3K subunit p85β abolished the Ephrin-A1/Fc-induced cell retraction in MEFs.

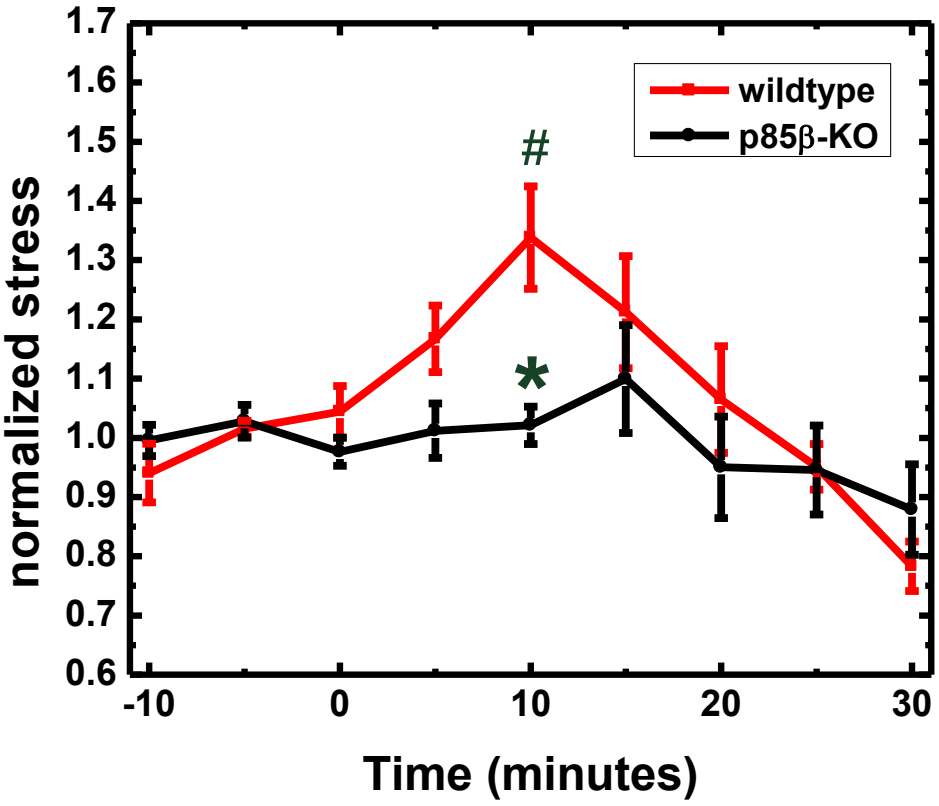


Figure 9. The traction stress exerted by wild type MEFs and p85β-/- MEFs treated with Ephrin-A1/Fc quantified over time. * indicates $p<0.05$ for comparison between p85β-/- and wild type MEFs at the same time points, and # indicates $p<0.05$ for comparison of the results after Ephrin-A1/Fc treatment with the value at time zero of the same cell line. The values were normalized with the mean values from the three time points before Ephrin-A1 treatment.

## 3.5 Ephrin-A1/Fc-Induced Effects in BAEC Monolayer

In the previous sections, the Ephrin-A1/Fc-induced cell retraction was probed at single cell level. The MEFs were used due to the availabilities of the p85 subunit knock out mice. In physiological condition, the cells are usually in contact with neighboring cells. Since it has been reported that Ephrins play important role in endothelial cell migration and vascular assembly in EC monolayer (Brantley-Sieders et al. 2004, Maekawa et al. 2003, Steinle et al. 2002), the monolayer of ECs was used to study the effect of Ephrin-A1/Fc.

### 3.5.1 Ephrin-A1/Fc Induces Morphological Change in EC Monolayer

As shown in Figure 10, Ephrin-A1/Fc-treated bovine aortic EC monolayer exhibited a morphological change over the 30-minute time course. The EC monolayer lost its attachment to the substrate and floated up as a sheet following 15 minutes after Ephrin-A1/Fc treatment (panels b vs. a). In contrast, EC monolayer stayed on the substrate stably when treated with control Fc fragment (panels f vs. e). Due to the detachment of the EC monolayer, the substrate deformation could not be measured (panel d), while that of the control group with Fc fragment treatment remained steady over time (panels g and h). These results indicate that Ephrin-A1/Fc has a strong effect on EC monolayer-substrate interaction and much less effect on EC-EC interaction.

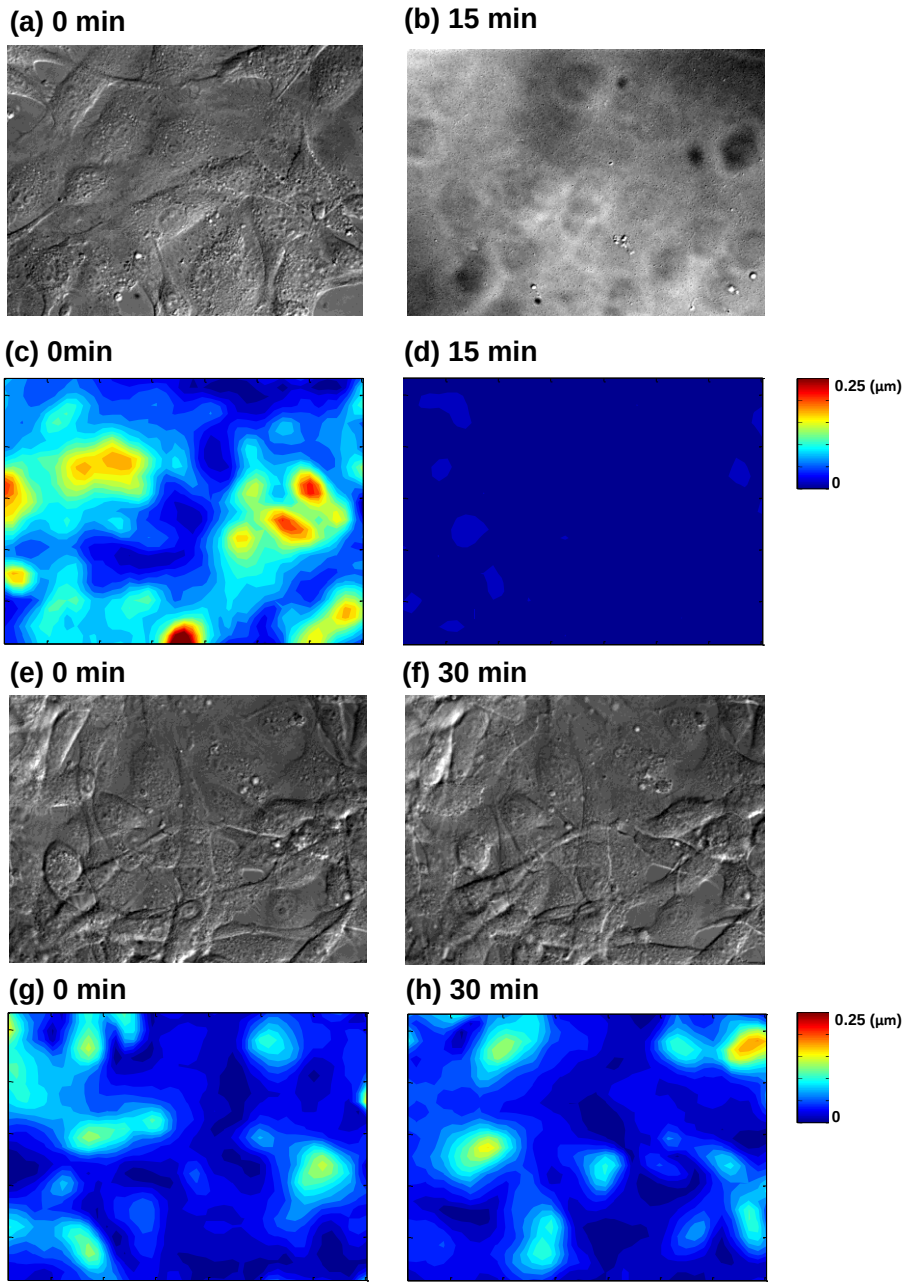


Figure 10. Effects of Ephrin-A1/Fc on EC monolayer. EC monolayer detachment induced by Ephrin-A1/Fc (panels a-d) and the lack of detachment in the control group with Fc fragment treatment (panels e-h) are shown. Bright-field images of EC monolayer are shown before (a) and 15 minutes after (b) treatment with Ephrin-A1/Fc (2μg/mL). The displacement fields of the embedded beads are also shown before (c) and 15 min after (d) the addition of Ephrin-A1/Fc (2μg/mL). The control group was also tracked before (panels e and g) and after (panels f and h) Fc fragment treatment. The color scales in the displacement fields indicate the magnitude of displacement.

### 3.5.2 Ephrin-A1/Fc Induces Change in Paxillin in BAEC monolayer

The results in Section 3.4.1 demonstrated that EC monolayer detached from the substrate after treatment with Ephrin-A1/Fc. To determine whether Ephrin-A1/Fc caused the reduction of focal adhesions in EC monolayer, paxillin was stained to determine the paxillin-containing focal adhesions before and after Ephrin-A1/Fc treatment in EC monolayer. In addition, β-catenin was stained to assess the changes of cell-cell junctions in EC monolayer. In Figure 11, the staining of paxillin-containing focal adhesions decreased after treatment with Ephrin-A1/Fc, while the β-catenin staining of intercellular junctions were largely retained. These results indicate that the Ephrin-A1/Fc induces a loss of focal adhesions in EC monolayer with less effect on intercellular junctions. That may provide the potential explanation for EC monolayer detachment as a sheet after the treatment with Ephrin-A1/Fc.

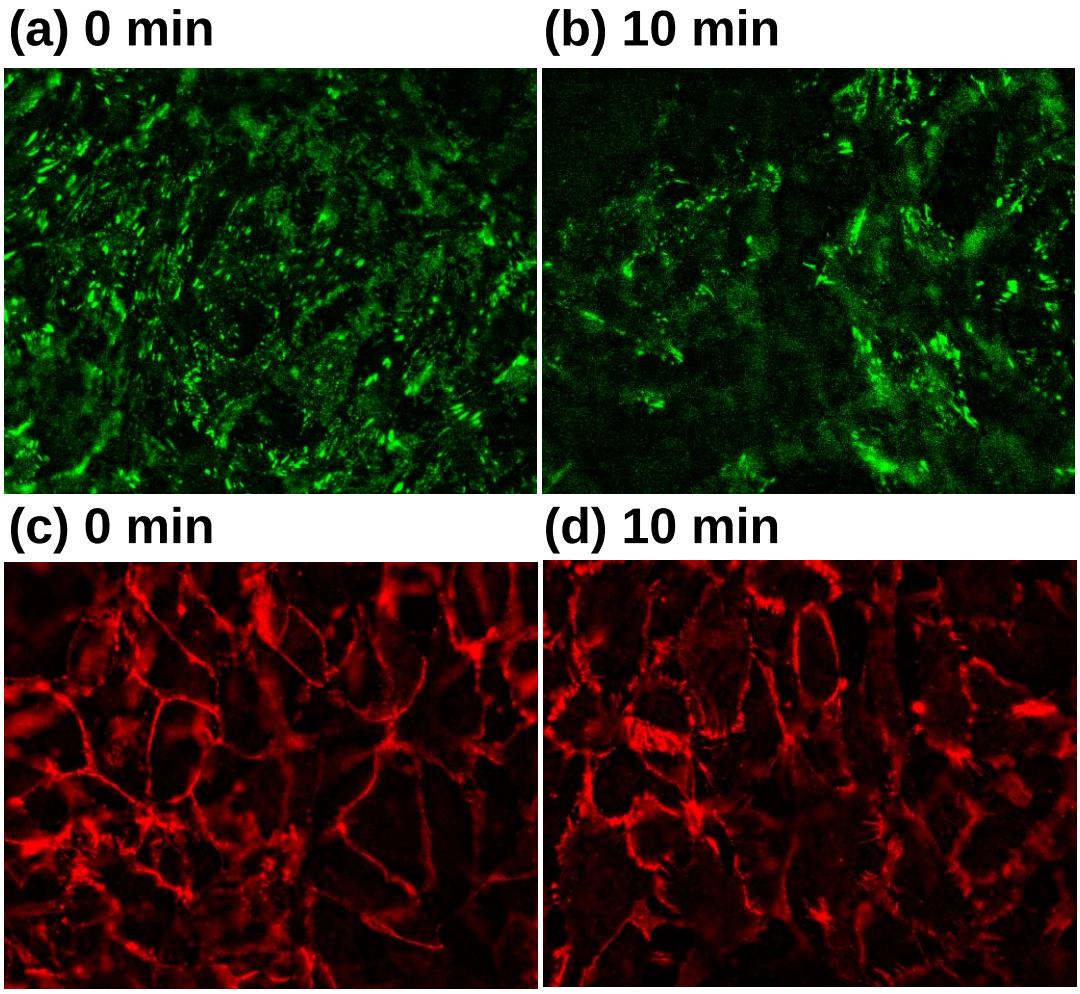


Figure 11. Effects of Ephrin-A1/Fc on paxillin-containing FAs and β-catenin-containing cell junctions. EC monolayers were treated with 2μg/mL Ephrin-A1/Fc for the indicated time periods. The cells were then fixed and immunocytochemistry was performed with primary antibodies against paxillin and β-catenin, followed by the incubation with FITC-conjugated secondary antibody. The immunostaining results were visualized via fluorescence microscopy. Ephrin-A1/Fc treatment caused a marked reduction of paxillin-containing focal adhesions (panels b vs. a), while the junctional β-catenin was not markedly affected (panels d vs. c). The images are representatives of four independent experiments.

# Chapter 4 Discussion

The results in Chapter 3 show that Ephrin-A1/Fc induces retraction of MEFs via a PI3K-dependent pathway in terms of a decrease in cell area and an increase in traction stresses exerted by the cells. The results on traction stress and PI3K extend our previous study on the morphological changes of MEFs and the phosphorylation of myosin light chain in the presence of Ephrin-A1/Fc (Fero 2008) in both biomechanical and biochemical directions. Previous studies have shown that the inhibition of PI3K is sufficient to prevent the Ephrin-induced cell retraction (Wong et al. 2004), and that RhoA activation is necessary for Ephrin-induced actin remodeling and cell retraction (Schmucker and Zipursky 2001). Furthermore, the RhoA activation was later reported in the downstream of PI3K signaling (Graupera et al. 2008, Saci and Carpenter 2005). The current findings indicate that PI3K signaling pathway is important for the regulation of cell retraction in MEFs in response to Ephrin-A1/Fc treatment. Class IA PI3K signaling is mediated through multiple heterodimer isoforms, including α, β, and δ. It has been shown that PI3Kα and β mediate different pathways modulated by Ephrin-A1/Fc (Marques et al. 2008, Tsukamoto et al. 2008). Our earlier study demonstrated that Ephrin-A1/Fc-induced cell contraction is mediated specifically by PI3K-p85β-dependent signaling to RhoA, MLC2, and the actin cytoskeleton (Fero 2008). Here I provide new evidence that such signaling pathway leads to the induction of traction stress generation, followed by cell contraction.

My results suggest that the Ephin-A1/Fc regulates differentially cell-substrate adhesion and cell-cell junction in EC monolayer (figures 10). After treatment with Ephrin-A1/Fc, the cell-substrate adhesion became weaker, while the cell-cell junctions remained essentially unchanged, and this change in stress balance resulted in a loss of attachment of the EC monolayer to the substrate. These results differ from the Ephrin-A1/Fc-induced cell retraction in single MEF with no cell-cell junctions. This can be explained as follows: although Ephrin-A1/Fc treatment weakens the MEF-substrate interaction by dephosphorylation and reduction of focal adhesion sites of paxillin (Fero 2011), the MEFs can remain in contact with the substrate in the absence of cell-cell junctions. In EC monolayers, however, the existence of cell-cell junctions leads to a shift in balance of force to lift the monolayer when it has weak adhesion to the substrate. The current findings are in concert with the concept that Eph receptor-Ephrin signaling is crucial to the process of cell migration and adhesion and leads to the formation of structured tissues in organisms (Holder and Klein 1999). It has also been shown that cells are unable to adhere to the Ephrin-A5-coated surface (Weinl et al. 2003, Zimmer G. et al. 2007) and that Ephrin causes the loss of cell adhesion to the substrate (Miao et al. 2000); these findings are in concert with our observation on Ephrin-A1/Fc-treated EC monolayer. Although the signaling pathway that regulates the Ephrin-A1/Fc-induced loss of cell adhesion has not been fully elucidated, several molecules were reported to be involved in Ephrin-A1/Fc-induced changes in cell adhesion. For example, it has been shown that Ephrin-A1 can dephosphorylate focal adhesion kinase (FAK) and paxillin (Miao et al. 2000). My findings, together with previous findings, indicate that Ephrin-A1 is able to

regulate the disassembly of FAs and control cell adhesion to substrate, and the consequential signaling event to modulate the homeostasis of cell adhesion.

In this study, the polyacrylamide gel substrate with a stiffness of 9 kPa was used. Interestingly, it has been shown that thrombin enhances the traction force in human umbilical vein endothelial cell (HUVEC) monolayer and causes the formation of intercellular gaps on stiffer substrate (Krishnan et al. 2011). In contrast, thrombin has much less effect on the traction forces in HUVEC monolayer and did not cause intercellular gap formation on softer substrate. These and other studies have shown the importance of substrate stiffness in affecting cellular responses (Discher et al. 2005). It is highly likely that the responses of cell contraction or adhesion to Ephrins will depend on the stiffness of substrates. Further studies will aim at the investigation of Ephrin-A1-regulation of cell-cell junctions and adhesions on substrates with different stiffness.

# Chapter 5 Conclusion

The Ephrin ligands and Eph family of receptor tyrosine kinases have been shown to play important roles through Eph-Ephrin signaling in regulating cell migration, polarization, and cell-substrate and cell-cell adhesions. The PI3K pathway has been reported to be important for the regulation of cell contraction induced by Ephrin-A1/Fc (Fero 2008). In my study, the changes of morphology, cell area, and traction stress exerted by the MEFs were investigated to determine the Ephrin-A1/Fc-induced cell retraction at a single cell level as well as in a monolayer. A new technique of three-dimensional traction force microscopy was employed to deduce the traction stresses exerted by the cells seeded on polyacrylamide deformable substrate with the use of a confocal microscope. The imaging processing programs coded with MATLAB was applied to track the displacement of fluorescent beads embedded in the substrate over a time course of 30 minutes following the treatment of Ephrin-A1/Fc, and the traction stress was calculated based on the finite element method. The results of this study show that Ephrin-A1/Fc induces cell retraction in MEFs and that the pik3R2 gene product, PI3K-p85β, plays a critical role in this regulation. Ephrin-A1 treatment caused an increase of traction stress exertion by MEFs at 10 minutes, followed by a decrease in cell area (maximum at 20-25 minutes). Furthermore, the effects of Ephrin-A1/Fc on cell-substrate adhesion and intercellular junctions in EC monolayer were investigated by immunostaining and fluorescence microscopy. My results on EC monolayer indicate that Ephrin-A1/Fc causes the reduction of paxillin-containing focal adhesions while having little effects on intercellular junction, and that this change in force balance may lead to the disruption of

cell-substrate interaction in response to the Ephrin-A1/Fc treatment.

In summary, my studies show that Ephrin-A1/Fc induces cell retraction and traction stresses generation in MEFs via a PI3K subunit p85β-dependent signaling pathway. Ephrin-A1/Fc also causes the disassembly of FAs and reduces cell adhesion to substrate in EC monolayer. My results show the role of Ephrin-A1/Fc as a regulator for cell attachment and interaction and its potential use as a chemo-repellent or repulsive coating material to guide cell migration and/or attachment pattern. Ephrin-A1/Fc may also be considered as a therapeutic tool for neovascularization in diseases such as retinopathy. Lastly, the application of the traction force microscopy technique provides a way to elucidate the biomechanical dynamics of cells in terms of their migrating and contractile activities in health and disease.

## References


Beauchamp A, Debinski W. 2012. Ephs and ephrins in cancer: Ephrin-A1 signalling. Seminars in Cell & Developmental Biology 23: 109-115.

Becker P, Waller H. 1986. Comparison of the Finite-Element Method and the Boundary Element Method for the Numerical-Calculation of Sound Fields. Acustica 60: 21-33.
Bereiter-Hahn J. 2005. Mechanics of crawling cells. Medical Engineering & Physics 27: 743-753.

Bershadsky AD, Balaban NQ, Geiger B. 2003. Adhesion-dependent cell mechanosensitivity. Annu Rev Cell Dev Biol 19: 677-695.

Bin Fang W, Brantley-Sieders DM, Hwang Y, Ham AJL, Chen J. 2008. Identification and functional analysis of phosphorylated tyrosine residues within EphA2 receptor tyrosine kinase. Journal of Biological Chemistry 283: 16017-16026.

Bochenek ML, Dickinson S, Astin JW, Adams RH, Nobes CD. 2010. Ephrin-B2 regulates endothelial cell morphology and motility independently of Eph-receptor binding. Journal of Cell Science 123: 1235-1246.

Brachmann SM, Yballe CM, Innocenti M, Deane JA, Fruman DA, Thomas SM, Cantley LC. 2005. Role of phosphoinositide 3-kinase regulatory isoforms in development and actin rearrangement. Mol Cell Biol 25: 2593-2606.

Brantley-Sieders DM, Caughron J, Hicks D, Pozzi A, Ruiz JC, Chen J. 2004. EphA2 receptor tyrosine kinase regulates endothelial cell migration and vascular assembly through phosphoinositide 3-kinase-mediated Rac1 GTPase activation. J Cell Sci 117: 2037-2049.

Brantley DM, et al. 2002. Soluble Eph A receptors inhibit tumor angiogenesis and progression in vivo. Oncogene 21: 7011-7026.

Buricchi F, Giannoni E, Grimaldi G, Parri M, Raugei G, Ramponi G, Chiarugi P. 2007. Redox Regulation of Ephrin/Integrin Cross-Talk. Cell Adhesion & Migration 1: 33-42.
Burton K, Taylor DL. 1997. Traction forces of cytokinesis measured with optically modified elastic substrata. Nature 385: 450-454.

Burton K, Park JH, Taylor DL. 1999. Keratocytes generate traction forces in two phases. Mol Biol Cell 10: 3745-3769.

Butler JP, Tolic-Norrelykke IM, Fabry B, Fredberg JJ. 2002. Traction fields, moments, and strain energy that cells exert on their surroundings. Am J Physiol Cell Physiol 282: C595-605.

Carter N, Nakamoto T, Hirai H, Hunter T. 2002. EphrinA1-induced cytoskeletal re-organization requires FAK and p130(cas). Nature Cell Biology 4: 565-573.

Castellvi J, Garcia A, de la Torre J, Hernandez J, Gil A, Xercavins J, Ramon y Cajal S. 2006. Ephrin B expression in epithelial ovarian neoplasms correlates with tumor differentiation and angiogenesis. Human Pathology 37: 883-889.

Chen J, Hicks D, Brantley-Sieders D, Cheng N, McCollum GW, Qi-Werdich X, Penn J. 2006. Inhibition of retinal neovascularization by soluble EphA2 receptor. Experimental Eye Research 82: 664-673.

Coate TM, Wirz JA, Copenhaver PF. 2008. Reverse signaling via a glycosyl-phosphatidylinositol-linked ephrin prevents midline crossing by migratory neurons during embryonic development in Manduca. Journal of Neuroscience 28: 3846-3860.

del Alamo JC, Meili R, Alonso-Latorre B, Bastounis E, Firtel RA, Lasheras JC. 2010. Three-Dimensional Forces Exerted by Migrating Amoeboid Cells. Biophysical Journal 98: 427a-427a.

del Alamo JC, Meili R, Alonso-Latorre B, Rodriguez-Rodriguez J, Aliseda A, Firtel RA, Lasheras JC. 2007. Spatio-temporal analysis of eukaryotic cell motility by improved force cytometry. Proc Natl Acad Sci U S A 104: 13343-13348.

Discher DE, Janmey P, Wang YL. 2005. Tissue cells feel and respond to the stiffness of their substrate. Science 310: 1139-1143.

Elson EL, Felder SF, Jay PY, Kolodney MS, Pasternak C. 1999. Forces in cell locomotion. Cell Behaviour: Control and Mechanism of Motility: 299-314.

Fero DJ. 2008. The Role of PI3K in Ephrin-A1 Induced Cell Retraction (Doctoral Dissertation). University of California, San Diego, La Jolla, CA, USA.

Fukushima K, Ueno Y, Inoue J, Kanno N, Shimosegawa T. 2006. Filopodia formation via a specific Eph family member and PI3K in immortalized cholangiocytes. American Journal of Physiology-Gastrointestinal and Liver Physiology 291: G812-G819.

Gale NW, Yancopoulos GD. 1997. Ephrins and their receptors: a repulsive topic: Cell and Tissue Research 290: 227-241.

Graupera M, et al. 2008. Angiogenesis selectively requires the p110alpha isoform of PI3K to control endothelial cell migration. Nature 453: 662-666.

Harris AK, Wild P, Stopak D. 1980. Silicone rubber substrata: a new wrinkle in the study of cell locomotion. Science 208: 177-179.

Hartshorne DJ, Ito M, Erdodi F. 1998. Myosin light chain phosphatase: subunit composition, interactions and regulation. Journal of Muscle Research and Cell Motility 19: 325-341.

Hjorthaug HS, Aasheim HC. 2007. Ephrin-A1 stimulates migration of CD8(+)CCR7(+) T lymphocytes. European Journal of Immunology 37: 2326-2336.

Holder N, Klein R. 1999. Eph receptors and ephrins: effectors of morphogenesis. Development 126: 2033-2044.

Hur SS, Zhao Y, Li YS, Botvinick E, Chien S. 2009. Live Cells Exert 3-Dimensional Traction Forces on Their Substrata. Cell Mol Bioeng 2: 425-436.

Kaverina I, Krylyshkina O, Gimona M, Beningo K, Wang YL, Small JV. 2000. Enforced polarisation and locomotion of fibroblasts lacking microtubules. Curr Biol 10: 739-742.

Kinch MS, Moore MB, Harpole DH. 2003. Predictive value of the EphA2 receptor tyrosine kinase in lung cancer recurrence and survival. Clinical Cancer Research 9: 613-618.

Krishnan R, et al. 2011. Substrate stiffening promotes endothelial monolayer disruption through enhanced physical forces. Am J Physiol Cell Physiol 300: C146-154.

Kuijper S, Turner CJ, Adams RH. 2007. Regulation of angiogenesis by Eph-Ephrin interactions. Trends in Cardiovascular Medicine 17: 145-151.

Lee J, Leonard M, Oliver T, Ishihara A, Jacobson K. 1994. Traction Forces Generated by Locomoting Keratocytes. Journal of Cell Biology 127: 1957-1964.

Li C, Hu Z, Li Y. 1993. Poisson's ratio in polymer gels near the phase-transition point. Phys Rev E Stat Phys Plasmas Fluids Relat Interdiscip Topics 48: 603-606.

Li S, Chen BPC, Azuma N, Hu YL, Wu SZ, Sumpio BE, Shyy JYJ, Chien S. 1999. Distinct roles for the small GTPases Cdc42 and Rho in endothelial responses to shear stress. Journal of Clinical Investigation 103: 1141-1150.

Maekawa H, Oike Y, Kanda S, Ito Y, Yamada Y, Suda T. 2003. Ephrin-B2 induces migration of endothelial cells through the PI3K pathway and promotes angiogenesis in adult vasculature. Circulation 108: 279-279.

Marques M, Kumar A, Cortes I, Gonzalez-Garcia A, Hernandez C, Moreno-Ortiz MC, Carrera AC. 2008. Phosphoinositide 3-kinases p110alpha and p110beta regulate cell cycle entry, exhibiting distinct activation kinetics in G1 phase. Mol Cell Biol 28: 2803-2814.

Miao H, Burnett E, Kinch M, Simon E, Wang BC. 2000. Activation of EphA2 kinase suppresses integrin function and causes focal-adhesion-kinase dephosphorylation. Nature Cell Biology 2: 62-69.

Miao H, Wei BR, Peehl DM, Li Q, Alexandrou T, Schelling JR, Rhim JS, Sedor JR, Burnett E, Wang BC. 2001. Activation of EphA receptor tyrosine kinase inhibits the Ras/MAPK pathway. Nature Cell Biology 3: 527-530.

Nasreen N, Mohammed KA, Lai Y, Antony VB. 2007. Receptor EphA2 activation with ephrinA1 suppresses growth of malignant mesothelioma (MM). Cancer Letters 258: 215-222.

Ogawa K, Pasqualini R, Lindberg RA, Kain R, Freeman AL, Pasquale EB. 2000. The ephrin-A1 ligand and its receptor, EphA2, are expressed during tumor neovascularization. Oncogene 19: 6043-6052.

Pandey A, Lazar DF, Saltiel AR, Dixit VM. 1994. Activation of the Eck Receptor Protein-Tyrosine Kinase Stimulates Phosphatidylinositol 3-Kinase Activity. Journal of Biological Chemistry 269: 30154-30157.

Pandey A, Shao HN, Marks RM, Polverini PJ, Dixit VM. 1995. Role of B61, the Ligand for the Eck Receptor Tyrosine Kinase, in Tnf-Alpha-Induced Angiogenesis. Science 268: 567-569.

Parri M, Buricchi F, Taddei ML, Giannoni E, Raugei G, Ramponi G, Chiarugi P. 2005. EphrinA1 repulsive response is regulated by an EphA2 tyrosine phosphatase. Journal of Biological Chemistry 280: 34008-34018.

Parri M, Buricchi F, Giannoni E, Grimaldi G, Mello T, Raugei G, Ramponi G, Chiarugi P. 2007. EphrinA1 activates a Src/focal adhesion kinase-mediated motility response leading to Rho-dependent actino/myosin contractility. Journal of Biological Chemistry 282: 19619-19628.

Pasquale EB. 2005. Eph receptor signalling casts a wide net on cell behaviour. Nat Rev Mol Cell Biol 6: 462-475.

Pelham RJ, Jr., Wang Y. 1997. Cell locomotion and focal adhesions are regulated by substrate flexibility. Proc Natl Acad Sci U S A 94: 13661-13665.

Pratt RL, Kinch MS. 2002. Activation of the EphA2 tyrosine kinase stimulates the MAP/ERK kinase signaling cascade. Oncogene 21: 7690-7699.

Riedl JA, Brandt DT, Battle E, Price LS, Clevers H, Bos JL. 2005. Down-regulation of Rap1 activity is involved in ephrinB1-induced cell contraction. Biochemical Journal 389:

465-469.

Saci A, Carpenter CL. 2005. RhoA GTPase regulates B cell receptor signaling. Mol Cell 17: 205-214.

Schmucker D, Zipursky SL. 2001. Signaling downstream of Eph receptors and ephrin ligands. Cell 105: 701-704.

Steinle JJ, Meininger CJ, Forough R, Wu G, Wu MH, Granger HJ. 2002. Eph B4 receptor signaling mediates endothelial cell migration and proliferation via the phosphatidylinositol 3-kinase pathway. Journal of Biological Chemistry 277: 43830-43835.

Tan JL, Tien J, Pirone DM, Gray DS, Bhadriraju K, Chen CS. 2003. Cells lying on a bed of microneedles: An approach to isolate mechanical force. Proceedings of the National Academy of Sciences of the United States of America 100: 1484-1489.

Tsukamoto K, Hazeki K, Hoshi M, Nigorikawa K, Inoue N, Sasaki T, Hazeki O. 2008. Critical roles of the p110 beta subtype of phosphoinositide 3-kinase in lipopolysaccharide-induced Akt activation and negative regulation of nitrite production in RAW 264.7 cells. J Immunol 180: 2054-2061.

Wang JHC, Lin JS. 2007. Cell traction force and measurement methods. Biomechanics and Modeling in Mechanobiology 6: 361-371.

Watanabe N, Kato T, Fujita A, Ishizaki T, Narumiya S. 1999. Cooperation between mDia1 and ROCK in Rho-induced actin reorganization. Nature Cell Biology 1: 136-143.
Weinl C, Drescher U, Lang S, Bonhoeffer F, Loschinger J. 2003. On the turning of Xenopus retinal axons induced by ephrin-A5. Development 130: 1635-1643.

Weiss P, Moscona A. 1958. Type-specific morphogenesis of cartilages developed from dissociated limb and scleral mesenchyme in vitro. J Embryol Exp Morphol 6: 238-246.

Wong EV, Kerner JA, Jay DG. 2004. Convergent and divergent signaling mechanisms of growth cone collapse by ephrinA5 and slit2. Journal of Neurobiology 59: 66-81.

Zhuang G, Hunter S, Hwang Y, Chen J. 2007. Regulation of EphA2 receptor endocytosis by SHIP2 lipid phosphatase via phosphatidylinositol 3-Kinase-dependent Rac1 activation. J Biol Chem 282: 2683-2694.

Zimmer G, Kastner B, Weth F, Bolz J. 2007. Multiple effects of ephrin-A5 on cortical neurons are mediated by Src family kinases. Journal of Neuroscience 27: 5643-5653.

Zimmer M, Palmer A, Kohler J, Klein R. 2003. EphB-ephrinB bi-directional endocytosis terminates adhesion allowing contact mediated repulsion. Nat Cell Biol 5: 869-878.